NANO LETTERS

2007
Vol. 7, No. 9
2897−2900

Colloidal Quantum Dots in All-Dielectric High-*Q* Pillar Microcavities

Matthias Kahl,[†] Tim Thomay,[†] Verena Kohnle,[†] Katja Beha,[†] Jörg Merlein,[†] Matthias Hagner,[†] Andreas Halm,[†] Jan Ziegler,[‡] Thomas Nann,[‡] Yuri Fedutik,[§] Ulrike Woggon,[§] Mikhail Artemyev,[||] Fabián Pérez-Willard,[⊥] Alfred Leitenstorfer,[†] and Rudolf Bratschitsch*,[†]

Department of Physics and Center for Applied Photonics, University of Konstanz, D-78464 Konstanz, Germany, School of Chemical Sciences and Pharmacy, University of East Anglia, Norwich NR4 7TJ, United Kingdom, Experimental Physics IIb, University of Dortmund, D-44221 Dortmund, Germany, Belarussian State University, 220080 Minsk, Belarus, and Carl Zeiss NTS GmbH, D-73447 Oberkochen, Germany

Received July 25, 2007; Revised Manuscript Received August 13, 2007

ABSTRACT

We have fabricated all-dielectric high-*Q* optical pillar resonators with embedded colloidal CdSe/ZnS quantum dots or rods as light emitters by focused ion beam milling. Three-dimensional light confinement and distinct pillar microcavity modes are observed. Results from a waveguide model for the mode patterns and their spectral positions are in excellent agreement with the experimental data. Cavities with elliptical cross sections show higher quality factors in the short axis direction than do circular resonators of the same cross-sectional area.

The efficient coupling of a single-electron to a single-photon system is one of the main challenges in current nanophotonics. Successful implementation is promising not only for new fundamental tests of quantum theory but also for technological applications. The current need for efficient, robust single-photon sources for quantum cryptography may serve as one example. After successful demonstrations with molecules,[1] atoms,[2] and diamond color centers,[3] semiconductor single-photon sources based on quantum dots have been demonstrated.[4] In recent years, optical cavities in the weak-coupling regime have been implemented to increase the light-matter interaction further via the Purcell effect.[5] Even strong coupling between an exciton of a self-assembled semiconductor quantum dot and a photon inside a high-*Q* optical resonator has recently been reported,[6−8] and this work marks the onset of true solid-state quantum optics experiments. Three types of optical cavities (photonic crystals, microdisks, and micropillars) have been used to achieve strong coupling. Until now, photonic crystal microresonators have exhibited the highest ratio of quality factor to mode volume. This Q/V ratio is an indicator of the strength of the light−matter interaction.[9] However, these high values have been achieved only with thin freestanding semiconductor membranes, which lack robustness. Microdisk resonators have ultrahigh *Q* values with large mode volumes. Unfortunately, coupling light modes in and out of this cavity type is difficult. Micropillar cavities, however, show well-collimated photon emission.[10] This feature renders them very attractive for real-world applications. For example, their narrow emission cone may lead to efficient coupling into fiber networks. Despite all of the success of III−V pillar microcavities, a number of challenges still remain. The deliberate positioning of a self-assembled quantum dot in both the vertical and lateral center of the cavity mode for optimum coupling to the light mode has not been solved. Therefore, the recent use of colloidal semiconductor nanocrystals for cavity quantum electrodynamics experiments has received considerable attention.[11] In principle, these quantum dots may be freely positioned on a surface by physical or chemical methods. Another problem of III−V pillars with the highest quality factors[12] is the degradation of the cavity mirrors in ambient air as a result of oxidation of the AlAs layers. In addition, one of the limiting factors for even higher *Q* values of III−V micropillar resonators is absorption in the Bragg mirrors.[12] Therefore, dielectric mirror materials with a high band gap would be preferable. Attempts to combine III−V quantum dots grown by molecular beam epitaxy (MBE) with dielectric mirrors have already been made.[13] However, this combination of materials and fabrication methods renders the fabrication process cumbersome.

* Corresponding author. E-mail: rudolf.bratschitsch@uni-konstanz.de.
[†] University of Konstanz.
[‡] University of East Anglia.
[§] University of Dortmund.
[||] Belarussian State University.
[⊥] Carl Zeiss NTS GmbH.

10.1021/nl071812x CCC: $37.00
Published on Web 08/28/2007

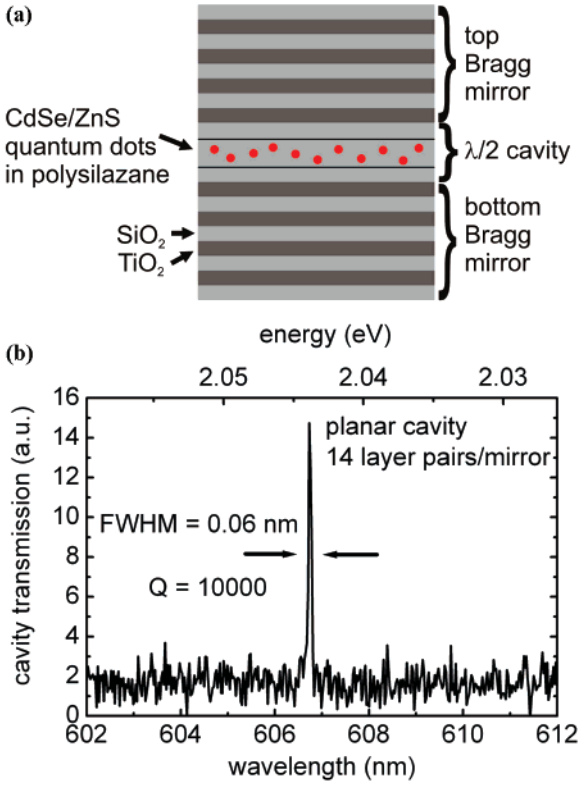

Figure 1. (a) Schematic drawing of a dielectric $\lambda/2$ planar cavity consisting of two SiO_2/TiO_2 Bragg mirrors and CdSe/ZnS quantum dots embedded in a polysilazane spacer layer. (b) Transmission spectrum of a planar cavity with 14 bottom and top Bragg layer pairs, showing a quality factor of 10 000.

In this letter, we present a new robust, all-dielectric, high-Q optical pillar microcavity with embedded colloidal semiconductor quantum dots. A planar dielectric cavity designed for a resonance wavelength of 605 nm is fabricated (Figure 1a) first by radio frequency (RF) magnetron sputtering of the bottom Bragg mirror. It consists of several alternating high and low refractive index TiO_2 and SiO_2 layer pairs with thicknesses of 61 and 104 nm, respectively. A Bragg mirror with high reflectivity in the visible part of the spectrum forms as a result of multiple interference. The $n(TiO_2) = 2.47$ and $n(SiO_2) = 1.46$ refractive indices guarantee a high contrast of $\Delta n = n(TiO_2)/n(SiO_2) = 1.69$, which is favorable for high mirror reflectivities. Subsequently, a SiO_2 layer is sputtered onto the bottom Bragg mirror, representing the first of three components of the central $\lambda/2$ cavity. In the second step, colloidal CdSe/ZnS core/shell semiconductor quantum dots dissolved in toluene are mixed with liquid polysilazane (NP 110-05, Clariant Ltd.) and spin coated onto the SiO_2 layer. Polysilazane solidifies in ambient air and transforms into a SiO_2 layer of 50 nm thickness. In this way, colloidal semiconductor quantum dots are embedded in all-dielectric surroundings. To complete the central cavity layer of exact $\lambda/2$ thickness (207 nm), additional SiO_2 is sputtered onto the solidified polysilazane layer with embedded quantum dots. Finally, the top TiO_2/SiO_2 Bragg mirror is deposited via sputtering. Figure 1b shows a white-light transmission spectrum through such a monolithic planar glass cavity with embedded CdSe/ZnS quantum dots and 14 top and bottom layer pairs each. The measured width of the transmission resonance is as small as 0.06 nm, which equals our spectrometer resolution. Hence, we derive a lower limit for the cavity Q factor of $Q = \Delta\lambda/\lambda = 10\,000$. This value is a factor of 50 higher than the previously reported record of $Q = 186$ for a planar SiO_2/TiO_2 resonator with colloidal semiconductor quantum dots embedded in a polymer.[14]

The planar dielectric cavity described above provides only 1D light confinement between the two Bragg mirrors. It may be viewed as a 1D photonic crystal. As a consequence, light can still leak out in lateral directions. In contrast, pillar microcavities exhibit 3D confinement due to laterally guided modes. To obtain high-quality resonators, such structures are milled into a planar cavity with a focused ion beam (FIB). A secondary electron microscope (SEM) image of a dielectric pillar resonator is shown in the inset of Figure 2. To characterize the optical properties and to demonstrate 3D light confinement inside a single-pillar microcavity, we perform stationary microphotoluminescence experiments in a confocal microscope setup equipped with a He-flow cryostate. The temperature is set to $T = 10$ K. A continuous wave solid-state laser at 532 nm is focused via a microscope objective (NA = 0.7) onto a single resonator to optically excite the quantum dot ensemble embedded in the pillar cavity. The emitted light is collected by the same objective and separated by a dichroic beam splitter before being fed into a spectrometer (1200 lines/mm, 0.06 nm resolution) with an attached Peltier-cooled CCD camera. Figure 2b shows the photoluminescence emission from a 3-μm-diameter micropillar cavity fabricated from a planar resonator with seven layer pairs per mirror. In addition to the spectral resolution, we also obtain 1D spatial information on the CCD image in the direction of the entrance slit of the monochromator (top of Figure 2b). Clearly, the mode patterns are different for higher-lying modes. The spatially integrated emission spectrum is shown at the bottom of Figure 2b, which consists of multiple resonances representing confined light modes in the optical resonator. The inhomogeneously broadened emission of the quantum dot ensemble outside the microcavity is centered at 630 nm and has a full-width at half-maximum (fwhm) of 28 nm. Hence, the fundamental mode of the pillar microcavity is close to the peak emission of the quantum dots. The density of nanocrystals in the active layer is on the order of 200 μm^{-2}. The spectral positions of the cavity resonances have been calculated by modeling the pillar cavity as a waveguide with an effective refractive index. First, the longitudinal modes in a planar cavity with the same layered structure as for the pillar resonator are calculated via the transfer-matrix method. In that way, we obtain the electric field amplitude in a direction perpendicular to the layers. An effective refractive index n_{eff} averaging over the entire pillar cavity is then obtained by weighting the refractive index at each point in space with the longitudinal electric field amplitude: $n_{eff} = \int n(z)\cdot|E(z)|^2/\max |E(z)|^2$. The electromagnetic field in the lateral direction may now be calculated by modeling the pillar microcavity as a homogeneous dielectric waveguide of cylindrical shape with an index of refraction n_{eff}. By solving the transverse wave

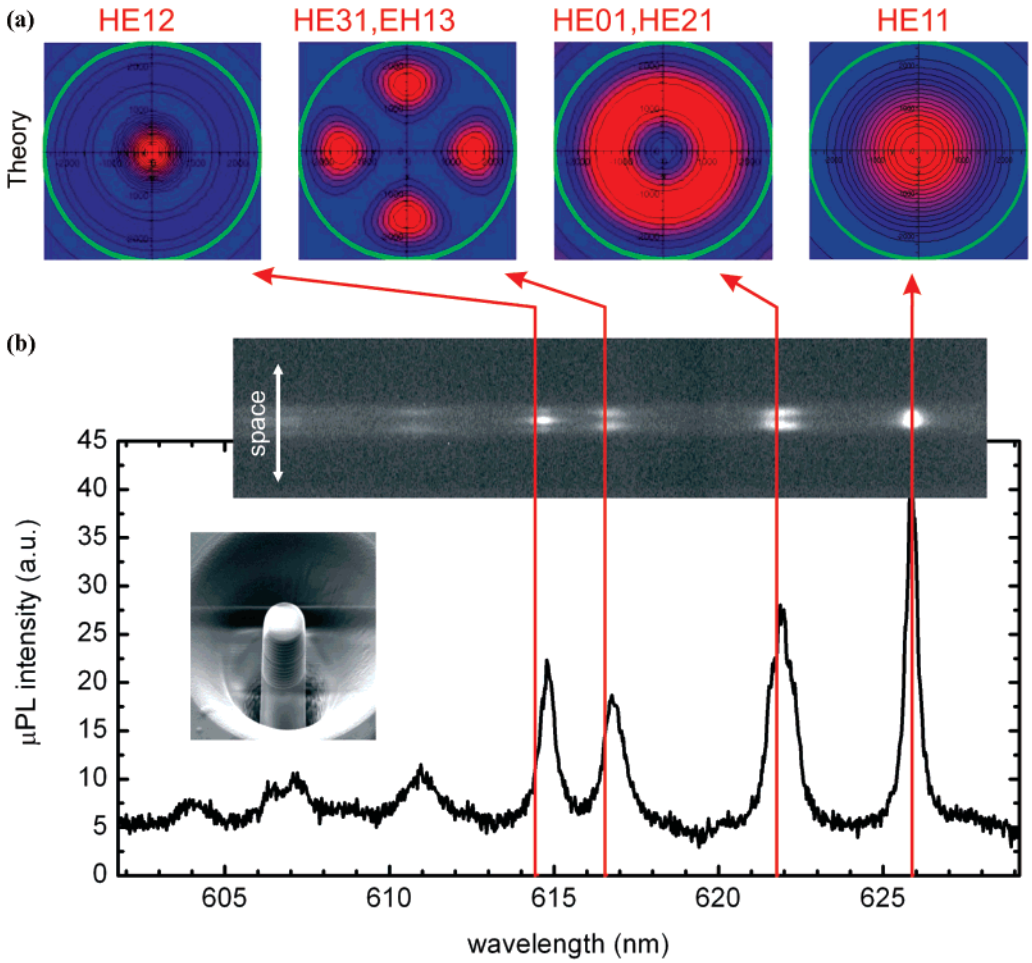

Figure 2. (a) Simulated pillar microcavity mode patterns of a 3-μm-diameter micropillar resonator. (b) Top: Spatio-spectrally resolved photoluminescence emission from colloidal CdSe/ZnS quantum dots in a 3-μm-diameter micropillar resonator. Bottom: Spatially integrated photoluminescence emission. Calculated mode positions are indicated by red lines. Inset: SEM image of the investigated pillar microcavity.

equation,[15] we finally determine the cavity modes of the pillar. The calculated mode positions indicated by red lines in Figure 2b are in excellent agreement with the values obtained in the experiment. We also obtain the spatial mode patterns depicted in Figure 2a from the simulations. Because the recorded photoluminescence emission provides us with 1D spatial resolution along the entrance slit of the spectrometer, the CCD image at the top of Figure 2b can be directly compared to a 1D vertical cut in the center of the calculated 2D mode patterns of Figure 2a. For example, the HE11 mode shows one intensity maximum, and the first excited modes (HE01, HE21) consist of two vertically displaced components. As is the case with the mode positions, calculated mode patterns are in excellent agreement with the experimental data.

To investigate the role of light confinement further in these microresonators, pillars with different diameters have been milled out of a planar cavity with seven layer pairs per mirror. Figure 3 shows the spectrally resolved photoluminescence (PL) emission from colloidal CdSe/ZnS quantum dots in two micropillar resonators with diameters of 1.52 μm and 920 nm, respectively. The PL emission unambiguously shows 3D light confinement. The fundamental mode of the resonator shifts to higher energies when

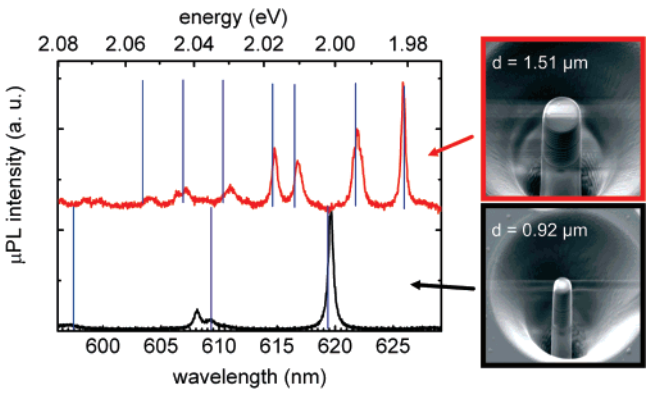

Figure 3. Left: Spectrally resolved photoluminescence emission from colloidal CdSe/ZnS quantum dots in circular micropillar resonators with 1.5 μm and 920 nm diameters. Vertical lines indicate calculated mode positions. Right: SEM images of circular micropillar resonators with 1.5 μm and 920 nm diameters.

the diameter of the pillar is reduced. In addition, the cavity mode spacing increases with smaller pillar diameters and hence demonstrates stronger light confinement.

Via FIB etching, we have also fabricated pillar resonators with elliptical cross sections (Figure 4a). This particular shape results in a splitting of the degenerate fundamental mode observed in a pillar cavity with a circular cross section into

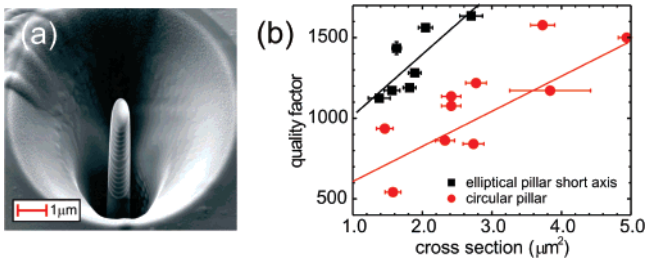

Figure 4. (a) SEM image of a micropillar resonator with an elliptical cross section. (b) *Q* factors of micropillar resonators with circular (red dots) and elliptical (black squares) cross sections. For the elliptical pillar, the *Q* values of modes polarized along the short axis are plotted.

two orthogonal modes with linear polarization. Surprisingly, we find a systematically higher *Q* factor for light polarization along the short axis of the elliptical pillar compared to that for circular ones (Figure 2b). This result is opposite of reports on micropost resonators based on the III−V material system, where the *Q* factor in direction of the long axis is favorable.[16,17] In III−V micropillars, the central λ-cavity layer is typically made of the high-index material. The cavity *Q* factor is governed by the angle of incidence of light entering a Bragg mirror from the central cavity layer. When the Brewster angle is reached, the Bragg mirrors loose their reflectivity in one polarization direction. As a consequence, the *Q* factor of the cavity drops dramatically. This effect leads to differences in the quality factor between the long and short axes of an elliptical III−V pillar resonator of 500%.[17] In our $\lambda/2$-dielectric cavity system, the central cavity layer is made of low-index material. Here, the Brewster angle is never reached, preventing the sudden drop in Bragg mirror reflectivity. In our case, the enhancement in the *Q* factor along the short axis of an elliptical pillar microcavity compared to that for a circular pillar with the same cross-sectional area (Figure 4b) stems from a different effect: if light is polarized along the short axis of an elliptical pillar, then it is laterally more confined than for a circular pillar of the same cross-sectional area. Therefore, the confined mode is less susceptible to light scattering due to surface roughness, which we consider to be the main limiting factor for the *Q* values of the current microresonators.

In summary, we have fabricated all-dielectric micropillar cavities with circular and elliptical cross sections containing colloidal CdSe/ZnS quantum dots. The high quality factors of the cavities are mainly due to embedding the semiconductor nanocrystals into a high band gap dielectric layer. We find systematically higher quality factors along the short axis of elliptical pillars compared to those for circular ones. In this study, we have excited an ensemble of semiconductor nanocrystals in a high-*Q* microcavity in order to characterize the mode structure. Placing single colloidal semiconductor quantum dots into the resonator will enable us to investigate quantum optics effects in the future. Presently, blinking and spectral diffusion of the nanocrystals limits the reliability of these single-electron hybrid devices. However, recent progress in photostability due to the fabrication of colloidal quantum dots with multiple protective shells is very promising.[18,19] Our photonic platform is suitable not only for semiconductor nanocrystals but also for embedding other nanoemitters of light, such as defect centers in diamond nanocrystals[20] or organic dye molecules.[21] This route may lead to a new class of robust active optical quantum devices based on single nanoobjects.

Acknowledgment. We gratefully acknowledge financial support by the Deutsche Forschungsgemeinschaft (DFG) through SFB 513, the Kompetenznetz Funktionelle Nanostrukturen Baden-Württemberg, the GRK 726 Materials and Concepts for Quantum Information Processing, and a grant from the Ministry of Science, Research and Arts, Baden-Württemberg.

References

(1) Brunel, C.; Lounis, B.; Tamarat, P.; Orrit, M. *Phys. Rev. Lett.* **1999**, *83*, 2722−2725.
(2) Kuhn, A.; Hennrich, M.; Rempe, G. *Phys. Rev. Lett.* **2002**, *89*, 67901−67904.
(3) Kurtsiefer, C.; Mayer, S.; Zarda, P.; Weinfurter, H. *Phys. Rev. Lett.* **2000**, *85*, 290−293.
(4) Michler, P.; Kiraz, A.; Becher, C.; Schoenfeld, W. V.; Petroff, P. M.; Zhang, L.; Hu, E.; Imamoglu, A. *Science* **2000**, *290*, 2282−2285.
(5) Gerard, J. M.; Sermage, B.; Gayral, B.; Legrand, B.; Costard, E.; Thierry-Mieg, V. *Phys. Rev. Lett.* **1998**, *81*, 1110−1113.
(6) Yoshie, T.; Scherer, A.; Hendrickson, A.; Khitrova, G.; Gibbs, H. M.; Rupper, G.; Ell, C.; Shchekin, O. B.; Deppe, D. G. *Nature* **2004**, *432*, 200−203.
(7) Peter, E.; Senellart, P.; Martrou, D.; Lemaitre, A.; Hours, J.; Gerard, J. M.; Bloch, J. *Phys. Rev. Lett.* **2005**, *95*, 67401−67404.
(8) Reithmaier, J. P.; Sek, G.; Löffler, A.; Hofmann, C.; Kuhn, S.; Reitzenstein, S.; Keldysh, L. V.; Kulakovskii, V. D.; Reinecke, T. L.; Forchel, A. *Nature* **2004**, *432*, 197−200.
(9) Vahala, K. J. *Nature* **2003**, *424*, 839−846.
(10) Rigneault, H.; Broudic, J.; Gayral B.; Gerard, J. M. *Opt. Lett.* **2001**, *26*, 1595−1597.
(11) Le Thomas, N.; Woggon, U.; Schöps, O.; Artemyev, M. V.; Kazes, M.; Banin, U. *Nano Lett.* **2006**, *6*, 557−561.
(12) Reitzenstein, S.; Hofmann, C.; Gorbunov, A.; Strauss, M.; Kwon, S. H.; Schneider, C.; Löffler, A.; Höfling, S.; Kamp, M.; Forchel, A. *Appl. Phys. Lett.* **2007**, *90*, 251109.
(13) Dalacu, D.; Potras, D.; Levebvre, J.; Poole, P. J.; Aers, G. C.; Williams, R. L. *Appl. Phys. Lett.* **2004**, *84*, 3235−3237.
(14) Li, Y. Q.; Steuerman, D. W.; Berezovsky, J.; Seferos, D. S.; Bazan, G. C.; Awschalom, D. D. *Appl. Phys. Lett.* **2006**, *88*, 193126.
(15) Love, J.; Snyder, A. *Optical Waveguide Theory;* Chapman & Hall: New York, 1983.
(16) Gayral, B.; Gerard, J. M.; Legrand, B.; Costard, E.; Thierry-Mieg, V. *Appl. Phys. Lett.* **1998**, *72*, 1421−1423.
(17) Darei, A.; Tahraoui, A.; Sanvitto, D.; Timpson, J. A.; Fry, P. W.; Hopkinson, M.; Guimares, P. S. S.; Vinck, H.; Whittaker, D. M.; Skolnick, M. S.; Fox, A. M. *Appl. Phys. Lett.* **2006**, *88*, 51113.
(18) Talapin, D. V.; Merks, I.; Götzinger, S.; Kornowski, A.; Benson, O.; Weller, H. *J. Phys. Chem. B* **2004**, *108*, 18826−18831.
(19) Aharoni, A.; Mokari, T.; Popov, I.; Banin, U. *J. Am. Chem. Soc.* **2006**, *128*, 257−264.
(20) Rabeau, J. R.; Chin, Y. L.; Prawer, S.; Jelezko, F.; Gaebel, T.; Wrachtrup, J. *Appl. Phys. Lett.* **2005**, *86*, 131926.
(21) Kiraz, A.; Ehrl, M.; Hellerer, Th.; Müstecaplioglu, Ö. E.; Bräuchle, C.; Zumbusch, A. *Phys. Rev. Lett.* **2005**, *94*, 223602.

NL071812X